Eur. Phys. J. D **10**, 279–283 (2000)

THE EUROPEAN PHYSICAL JOURNAL D

EDP Sciences

Spontaneous alloying of tin atoms into nanometer-sized gold clusters and phase stability in the resultant alloy clusters

H. Yasuda[1,2,a] and K. Furuya[2]

[1] Research Center for Ultra-High Voltage Electron Microscopy, Osaka University, Yamadaoka, Suita, Osaka 565–0871, Japan
[2] National Research Institute for Metals, Sakura, Tsukuba, Ibaraki 305–0003, Japan

Received 2 August 1999 and Received in final form 8 November 1999

Abstract. Alloying behavior and phase stability has been studied *in situ* by transmission electron microscopy using clusters in the Au–Sn system. When tin atoms are vapor-deposited onto nm-sized gold clusters, rapid dissolution of tin atoms into gold clusters takes place and as a result Au-rich solid solution, amorphous-like Au–Sn alloy and AuSn compound clusters are formed depending upon the concentration of tin. The remarkable enhancement of solubility has been observed in Au-rich solid solution and AuSn compound. It becomes more difficult to form two phases in the interior of individual clusters even if the composition of alloy clusters falls in the two-phase region in the phase diagram for the bulk alloy and as a result amorphous-like phase is stabilized in nm-sized Au–Sn alloy clusters.

PACS. 61.16.-d Electron, ion, and scanning probe microscopy – 36.40.-c Atomic and molecular clusters – 64.70.-p Specific phase transitions

1 Introduction

Small particles in the size range from a few to several nanometer (nm) often exhibit physical and chemical properties and phase stability that are significantly different from those of the corresponding bulk materials (hereafter such small particles are designated as clusters) [1,2]. It was recently found that in nm-sized clusters rapid spontaneous dissolution of solute atoms takes place and homogeneously alloyed clusters are formed when solute atoms are vapor-deposited onto the clusters kept at ambient temperature [3–7]. On the other hand, it is well-known that phase transition temperatures of nm-sized clusters are significantly depressed compared to those of the corresponding bulk materials. For example, such phase transition temperatures as the melting point or the order-disorder critical temperature are markedly reduced with decreasing size of clusters [8–12]. However, studies on the phase stability in nm-sized binary alloy clusters are few [13–16].

In this work, alloying behavior of tin atoms into nm-sized gold clusters has been studied *in situ* by transmission electron microscopy (TEM). At the same time, the stability in the resultant Au–Sn alloy clusters has been also examined with emphasis on the study of the difference in the stability between the bulk materials and the corresponding nm-sized clusters.

[a] e-mail: yasuda@uhvem.osaka-u.ac.jp

2 Experimental procedures

Preparation of gold clusters and subsequent vapor-deposition of tin onto gold clusters was carried out using a double-source evaporator installed in the specimen chamber of an electron microscope. Using the evaporator, gold was first evaporated onto an amorphous carbon film, and nm-sized gold clusters were produced. Tin was then evaporated from the second source onto gold clusters on the film kept at ambient temperature. Changes in the structure and chemical composition of clusters associated with tin deposition were studied *in situ*. The chemical composition of individual clusters on the film was analyzed by energy dispersive X-ray spectroscopy (EDS). The analyses were carried out using an electron probe of approximately 1 nm in diameter. The characteristic X-rays of gold and tin were acquired using an ultrathin window X-ray detector. The background was simulated by the curve fitting, and then subtracted. The chemical composition of clusters was calculated from the intensity ratio of AuLα_1 to SnLα_1 peak, using sensitivity factors. The microscope used was a Hitachi HF-2000 TEM equipped with a field emission gun, operating at an accelerating voltage of 200 kV. The base pressure in the specimen chamber was below 5×10^{-7} Pa.

3 Results

A typical sequence of spontaneous alloying of tin atoms into gold clusters is shown in Figure 1. Figures 1a and 1a′ show a bright-field image (BFI) of as-produced

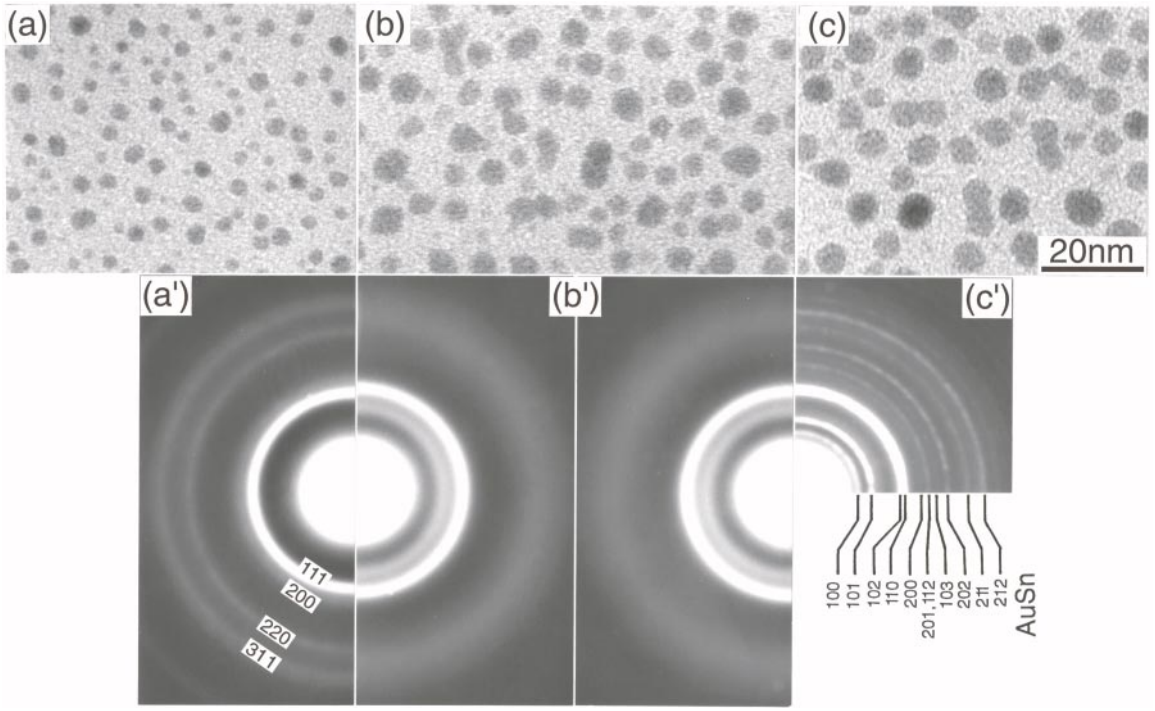

Fig. 1. A typical sequence of spontaneous alloying of tin atoms into gold clusters kept at ambient temperature. (a) A BFI of as-produced gold clusters on a supporting film and (a′) the corresponding SAED. (b) A BFI of clusters after tin deposition and (b′) the corresponding SAED. (c) A BFI of the clusters after additional deposition of tin and (c′) the corresponding SAED.

gold clusters on a supporting film and the corresponding selected area electron diffraction pattern (SAED), respectively. The mean diameter of initial gold clusters is $3 \sim 4$ nm. The Debye-Scherrer rings in the SAED can consistently be indexed as those of fcc gold. Figures 1b and 1b′ show a BFI of clusters after tin deposition and the corresponding SAED, respectively. The cluster size has increased to $5 \sim 6$ nm in mean diameter. EDS of the sample shown in Figure 1b revealed that, after the tin deposition, the material on the supporting film contained approximately 40 at%Sn. In the SAED (Fig. 1b′), two kinds of diffuse rings are recognized. The value of the scattering vector ($K = (4\pi \sin\theta)/\lambda$) for the first diffuse ring is approximately 22.5 nm^{-1}. Similarly, the value of the scattering vector for the second diffuse ring is approximately 28.0 nm^{-1}. This fact indicates that vapor-deposited tin atoms came in contact with gold clusters and dissolved quickly into the clusters to form amorphous-like Au–Sn alloy clusters, and this alloying induces the formation of mixture of two kinds of amorphous-like alloy phases in clusters. Stable phases in the Au $\sim$ 40 at%Sn bulk material are Au_5Sn and AuSn [17]. Namely, in Au $\sim$ 40 at%Sn alloy clusters of $5 \sim 6$ nm in mean diameter, stable phases in the corresponding bulk material are not produced. Figures 1c and 1c′ show a BFI of clusters after additional deposition of tin and the corresponding SAED, respectively. After this second deposition of tin, the mean size of the clusters has increased to approximately $7 \sim 8$ nm in mean diameter. As illustrated in the SAED (Fig. 1c′), the Debye-Scherrer rings can be consistently indexed as those of AuSn, which has the $B8_1$ structure of the space-group $P6_3/mmc$ with lattice constants of $a_0 = 0.43_2$ nm and $c_0 = 0.55_2$ [18]. It is considered that after the second deposition of tin the concentration of tin in the Au–Sn alloy clusters has reached to a value close to the stoichiometric composition of AuSn.

All these observations shown in Figure 1 indicate that when tin atoms are vapor-deposited onto nm-sized gold clusters, rapid dissolution of tin atoms into gold clusters takes place and as a result amorphous-like Au–Sn alloy and AuSn compound clusters are successively formed.

The atomic structure of alloy clusters with compositions of 18, 32, 40, 46 and 59 at%Sn, all of which fall in the two-phase region in the phase diagram for the bulk alloy, were examined by high resolution electron microscopy. Figure 2 shows examples of high-resolution images (HRIs) taken from these alloy clusters, with the corresponding EDS spectra. The EDS spectra were measured at the region encircled in HRIs in Figure 2.

Figure 2a shows an HRI of an Au–18 at%Sn alloy cluster and the corresponding EDS spectrum. The diameter of the cluster is approximately 5 nm. In Figure 2a, there appear lattice fringes with a spacing of 0.24 nm. The spacing is very close to the (111) lattice spacing of fcc gold. From the image, it is evident that the cluster is a multiply twined crystal in a nearly five-fold orientation; the incident beam is along the [110] direction. This fact suggests that the cluster is an Au–Sn solid solution and that the solid solubility of tin in nm-sized gold clusters amounts to at least 18 at%Sn, which is much higher than that in bulk gold (*i.e.*, $\sim$ 3 at%Sn at room temperature and 6.8 at%Sn as the maximum at approximately 753 K).

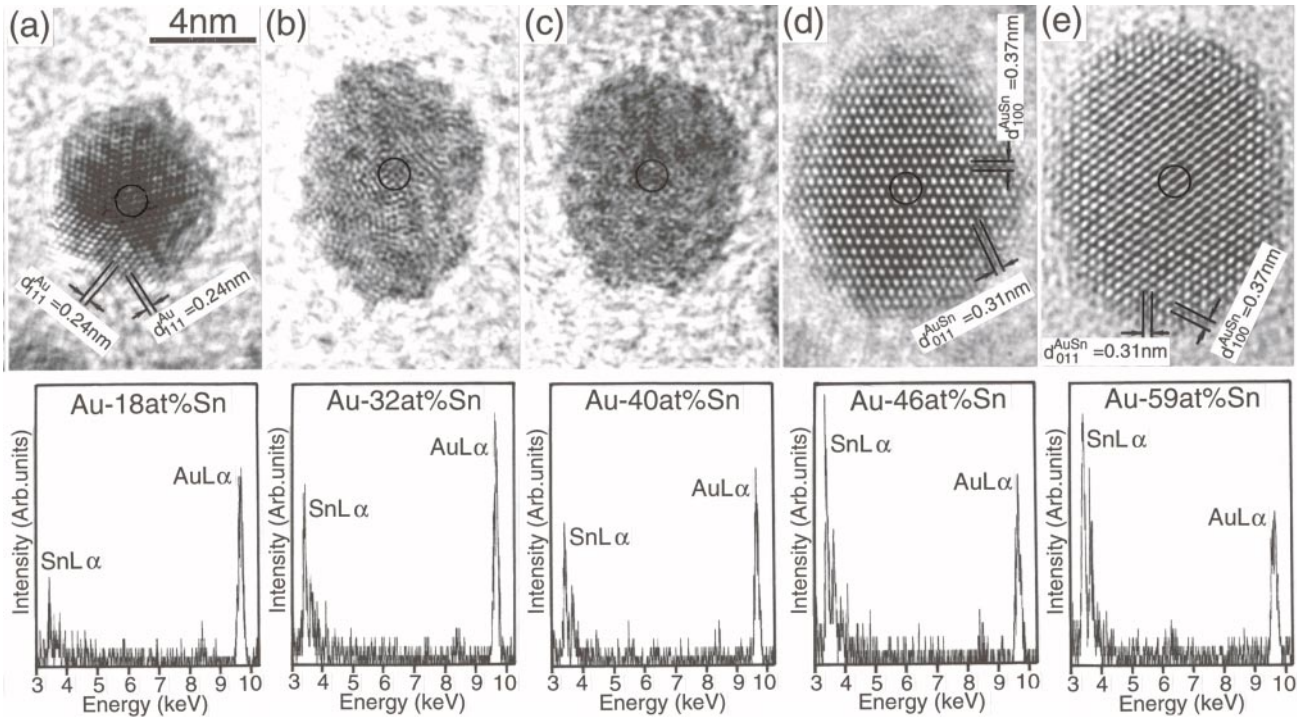

Fig. 2. HRIs of alloy clusters and the EDS spectra measured at the region encircled. (a) An example of Au–18 at%Sn alloy clusters. (b) An example of Au–32 at%Sn alloy clusters. (c) An example of Au–40 at%Sn alloy clusters. (d) An example of Au–46 at%Sn alloy clusters. (e) An example of Au–59 at%Sn alloy clusters.

HRIs taken from Au–32 at%Sn and Au–40 at%Sn alloy clusters are shown in Figures 2b and 2c, respectively. The diameter of these clusters is approximately 6 nm. Both clusters exhibit a contrast similar to the salt and pepper contrast characteristic of amorphous materials. This result is consistent with the result shown in Figure 1b′ where diffuse rings are recognized in the SAED. This observation indicates that an amorphous-like phase is produced in 6 nm-sized alloy clusters in the composition range from 32 to 40 at%Sn.

Figures 2d and 2e show HRIs of approximately 8 nm-sized AuSn compound clusters with different chemical compositions. Both compound clusters are single crystalline. The 0.31 nm and 0.37 nm-spaced fringes in the images are the (011) and (100) lattice fringes of AuSn, respectively. These fringes make an angle of 66 degrees to each other, showing that the incident beam direction is along the [011] of AuSn. EDS spectra in Figures 2d and 2e indicate that tin concentrations of clusters are 46 at%Sn (which is by $\sim$ 4 at% lower than the stoichiometric composition of AuSn) and 59 at%Sn (which is by $\sim$ 9 at% higher than the stoichiometric composition of AuSn), respectively. From this result, it is evident that remarkable enhancement of solubility has been induced in AuSn compound clusters, as compared with that in the corresponding bulk AuSn (*i.e.*, a maximum value of the deviation from the stoichiometric composition of AuSn is +0.5 at%Sn at 582 K).

In the present experiments, total X-ray counts under either the AuLα_1 or SnLα_1 peaks are several hundreds and are very low, because only approximately 200–300 atoms are contained in the analyzed region. It was confirmed from the preliminary experiments that the compositional error depending on total X-ray counts is within $\pm$2 at%Sn. On the other hand, the error of compositions determined by measurements repeated at three close positions in the individual clusters was less than $\pm$1 at%Sn. Consequently, it is expected that the total error of compositions was within $\pm$3 at%Sn.

It is considered that the compositions given by EDS measurements are influenced by a compositional inhomogeneity in the individual clusters. It is known that surface segregation which is one of the typical inhomogeneities occurs even in clusters. Due to the large difference of surface tensions between gold and tin (*i.e.*, the surface tensions are $\sim 1\,400$ mJ m^{-2} for gold and ~ 560 mJ m^{-2} for tin [19]), it is expected that a large occupation of surface sites by tin atoms is induced. In the present experiments, an electron probe used to measure the chemical composition in clusters is approximately 1 nm in diameter. The electron beam is not diverged in the cluster which is several nm in thickness. Therefore, the chemical composition was measured from a columnar-shaped region (with 1 nm diameter and heights which corresponds to cluster diameters). In the columnar-shaped region through individual clusters with diameters from approximately 5 to 8 nm, atomic fraction of the first layer of the clusters surface is approximately 5–9%. Consequently, it is estimated that the chemical compositions in the interior of clusters with diameters of approximately 5–8 nm are by 2–7 at%Sn

lower than those obtained by EDS measurements, even if surface segregation by which 90% of the first surface layer is covered by tin atoms occurs in clusters.

It is shown that the results on an enhanced solubility in clusters are not influenced by the error of compositions measured or by inhomogeneities in the individual clusters such as surface segregation.

4 Discussion

Through the present experiment, it becomes evident that when tin atoms are vapor-deposited onto nm-sized gold clusters, rapid dissolution of tin atoms into gold clusters takes place and as a result of this, Au-rich fcc solid solution alloy, amorphous-like Au–Sn alloy and AuSn compound clusters are formed depending upon the concentration of tin. The solid solubility of tin increases significantly in clusters compared with that for the corresponding bulk materials. The remarkable enhancement of solubility has been observed also in AuSn compound.

A discussion will be made on the magnitude of temperature rise in clusters, in order to see whether or not such rapid dissolution is ascribed to any temperature rise in clusters. Model calculations were carried out on the temperature of clusters that would be induced by (1) electron beam heating, (2) heat of condensation, (3) heat of mixing, and (4) impingement of flying solute atoms with a kinetic energy of the order of $2kT$. Using the value of 1.5×10^{20} e m^{-2}s^{-1} for the electron flux in the present experiments, a value of 8 K is obtained by calculation for the temperature rise in nm-sized gold clusters. It seems reasonable to estimate that the magnitude of the temperature rise in gold clusters due to the beam heating is of the order of 10 K. This estimation is not so different from that by Takayanagi *et al.* [20]. The cohesive energy and atom-accumulation rate of tin for a gold cluster are 303 kJ mol^{-1} [21] and 20 atom s^{-1}, respectively. With the use of these values, a value of 2.5×10^{-3} K is obtained by calculation for the temperature rise in clusters due to the heat of condensation. A value of the heat of mixing for an AuSn alloy at 300 K is -30.5 kJ mol^{-1} [22] and the atom-accumulation rate is 20 atom s^{-1}. Using these values, a value of 7.0×10^{-4} K is obtained by calculation for the temperature rise in clusters due to the heat of mixing. When a tin atom directly impinges on a gold cluster and is incorporated into the cluster, the kinetic energy of the tin atom will be converted into heat in the cluster. The average kinetic energy of tin atoms is given by $2kT$, where k is the Boltzmann constant. The value for T in the above equation is 505 K (the melting temperature of tin). The rate of direct impingement of tin atoms on a gold cluster was approximately 7 atom s^{-1}. With the use of these values, a value of 1.5×10^{-4} K is obtained by calculation for the temperature rise in clusters due to an impingement of flying tin atoms. Of the four items mentioned above, the beam heating brings about the highest temperature rise (*i.e.*, ~ 10 K). It was concluded that the spontaneous alloying in clusters is not an artifact originating from the temperature rise in clusters but is an intrinsic property of clusters.

In nm-sized alloy clusters, it becomes more difficult to form two phases in the interior of individual clusters even if the composition of alloy clusters falls in the two-phase region in the phase diagram for the bulk alloy and as a result amorphous-like phase is stabilized. It is considered that short range structures which consist of unit cells of solid solutions or compounds distribute homogeneously, because remarkably stable phases are not present in the two-phase region. It is now well-known that in nm-sized clusters, the lattice itself becomes elastically soft to a great extent [23,24]. It is then expected the lattice distortion induced by dissolution of solute atoms could be relaxed rather easily than in bulk materials. Consequently, it seems reasonable to consider such atomic arrangements that are under the control of only chemical interactions among constituent atoms preferentially appear in nm-sized clusters. In this case, if the concentration of solute atoms (tin) is small in the solvent matrix (gold), a solid solution with an enhanced solubility will be formed. Similarly at compositions slightly deviated from the stoichiometric composition of a very stable intermediate phase (AuSn), an enhanced solubility will be achieved. On the other hand, if the composition is so high (or so deviated from the stoichiometry) that it falls in the middle of a two-phase region in the bulk phase diagram, there will be a possibility that amorphous-like phase which exhibits less defined long-range periodicity of atom arrangement is formed. A possible structure of such a phase may be a mixture of unit cells in the neighbouring stable phases (*i.e.*, in the present example, a mixture of unit cells of an fcc solid solution and the AuSn compound). Namely, in this case, it is expected that such a phase with the structure where the chemical environment around each individual atom is much valued as compared to the geometrical regularity (or geometrical constraint) of atom arrangement will appear. Our preliminary experiment on thermal stability in such an amorphous-like phase, which was carried out in Au–Sn alloy clusters, has revealed that the amorphous-like phase directly transforms to a liquid phase without any crystallizations with increasing temperature, and then the inverse transformation takes place with decreasing temperature. Details will be published in a separate paper.

In previous articles, it was reported that a similar amorphization by solid-state reaction in multilayered ultra-thin metallic films occurs in a restricted thin interface region at reduced temperatures [25,26]. However, it is considered that the stability of the amorphous-like phase in alloy clusters observed in the present work is different from that of the amorphous phase formed by interface reaction in multilayered thin films, because the former is stable thermally but the latter crystallizes with increasing temperature. It is suggested that the amorphous-like phase in alloy clusters is in equilibrium states, whereas the amorphous phase formed in multilayered thin films is in non-equilibrium states. Based on these discussions, it seems that the formation of amorphous-like phase and the increase of solid solubility observed here may be an

intrinsic feature of the phase stability in nm-sized alloy clusters. A systematic study on the structure and chemical composition of nm-sized alloy clusters are in progress in our laboratory.

5 Conclusion

Alloying behavior and phase stability has been studied *in situ* by TEM using clusters in the Au–Sn system. When tin atoms are vapor-deposited onto nm-sized gold clusters, rapid dissolution of tin atoms into gold clusters takes place and as a result Au-rich solid solution, amorphous-like Au–Sn alloy and AuSn compound clusters are formed depending upon the concentration of tin. The remarkable enhancement of solubility has been observed in Au-rich solid solution and AuSn compound. In case the composition of alloy clusters fall in the two-phase region of the phase diagram for the bulk alloy, an amorphous-like phase is stabilized in nm-sized alloy clusters.

This work is, in part, supported by "Research for the Future" Program, JSPS #96P00305, and also in part, by the Ministry of Education, Science, Sports and Culture under Grant-in-Aid for Scientific Research.

References

1. W.P. Halperin, Rev. Mod. Phys. **58**, 533 (1986).
2. R.P. Andres, R.S. Averback, W.L. Brown, L.E. Brus, W.A. Goddard, A. Kaldor, S.G. Louie, M. Moscovits, P.S. Peercy, S.J. Riley, R.W. Siegel, F. Spaepen, Y. Wang, J. Mater. Res. **4**, 704 (1989).
3. H. Mori, M. Komatsu, K. Takeda, H. Fujita, Philos. Mag. Lett. **63**, 173 (1991).
4. H. Yasuda, H. Mori, Phys. Rev. Lett. **69**, 3747 (1992).
5. H. Yasuda, H. Mori, Z. Phys. D **31**, 209 (1994).
6. H. Mori, H. Yasuda, T. Kamino, Philos. Mag. Lett. **69**, 279 (1994).
7. H. Yasuda, H. Mori, Z. Phys. D **40**, 140 (1997).
8. M. Takagi, J. Phys. Soc. Jpn **9**, 359 (1951).
9. J.R. Sambles, Proc. R. Soc. Lond. A **324**, 339 (1971).
10. G.L. Allen, R.A. Bayles, W.W. Gile, W.A. Jesser, Thin Solid Films **144**, 297 (1986).
11. T. Castro, R. Reinfenberger, E. Choi, R.P. Andres, Phys. Rev. B **42**, 8548 (1990).
12. H. Yasuda, H. Mori, Z. Phys. D **37**, 181 (1996).
13. L.S. Palatnik, B.T. Boiko, Phys. Metals Metallog. **11**, 119 (1961).
14. G.L. Allen, W.A. Jesser, J. Cryst. Growth **70**, 546 (1984).
15. H. Yasuda, H. Mori, Philos. Mag. A **73**, 567 (1996).
16. H. Mori, H. Yasuda, Mater. Sci. Eng. A **217/218**, 244 (1996).
17. H. Okamoto, T.B. Massalski, *Binary Alloy Phase Diagrams*, edited by T.B. Massalski *et al.* (ASM, Metals Park, OH, 1986).
18. P. Villars, L.D. Calvert, *Pearson's Handbook of Crystallographic Data for Intermetallic Phases* (ASM, Metals Park, OH, 1985).
19. J.M. Blakely, *Introduction to the Properties of Crystal Surfaces* (Pergamon, 1973).
20. M. Mitome, Y. Tanishiro, K.Takayanagi, Z. Phys. D **12**, 45 (1989).
21. C. Kittel, *Introduction to Solid State Physics*, 2nd edn. (John Wiley and Sons, NY, 1956).
22. R. Hultgren, P.D. Desai, D.T. Hawkins, M. Gleiser, K.K. Kelley, *Selected Values of the Thermodynamic Properties of Binary Alloys* (American Society for Metals, OH, 1973).
23. J. Harada, K. Ohshima, Surf. Sci. **106**, 51 (1981).
24. U. Buck, R. Krohne, Phys. Rev. Lett. **73**, 947 (1994).
25. M. Seyffert, A. Siber, P. Ziemann, Phys. Rev. Lett. **67**, 3792 (1991).
26. M. Seyffert, A. Siber, P. Ziemann, Thin Solid Films **208**, 197 (1992).